

## Supplementary Information

for

### Correlation of the ratio of metallic to oxide species with activity of PdPt catalysts for methane oxidation

Tang Son Nguyen<sup>a,b\*</sup>, Paul McKeever<sup>a</sup>, Miryam Arredondo-Arechavala<sup>c</sup>, Yi-Chi Wang<sup>d</sup>,  
Thomas J. A. Slater<sup>e</sup>, Sarah J. Haigh<sup>d</sup>, Andrew M. Beale<sup>f\*</sup>, Jillian M. Thompson<sup>a\*</sup>

<sup>a</sup>School of Chemistry and Chemical Engineering, Queen's University, Belfast BT9 5AG,  
Northern Ireland, UK

<sup>b</sup>Faculty of Biotechnology, Chemistry and Environmental Engineering, PHENIKAA  
University, Hanoi 10000, Vietnam

<sup>c</sup>Centre for Nanostructured Media, School of Mathematics and Physics, Queen's  
University Belfast, University Road, Belfast BT7 1NN, United Kingdom

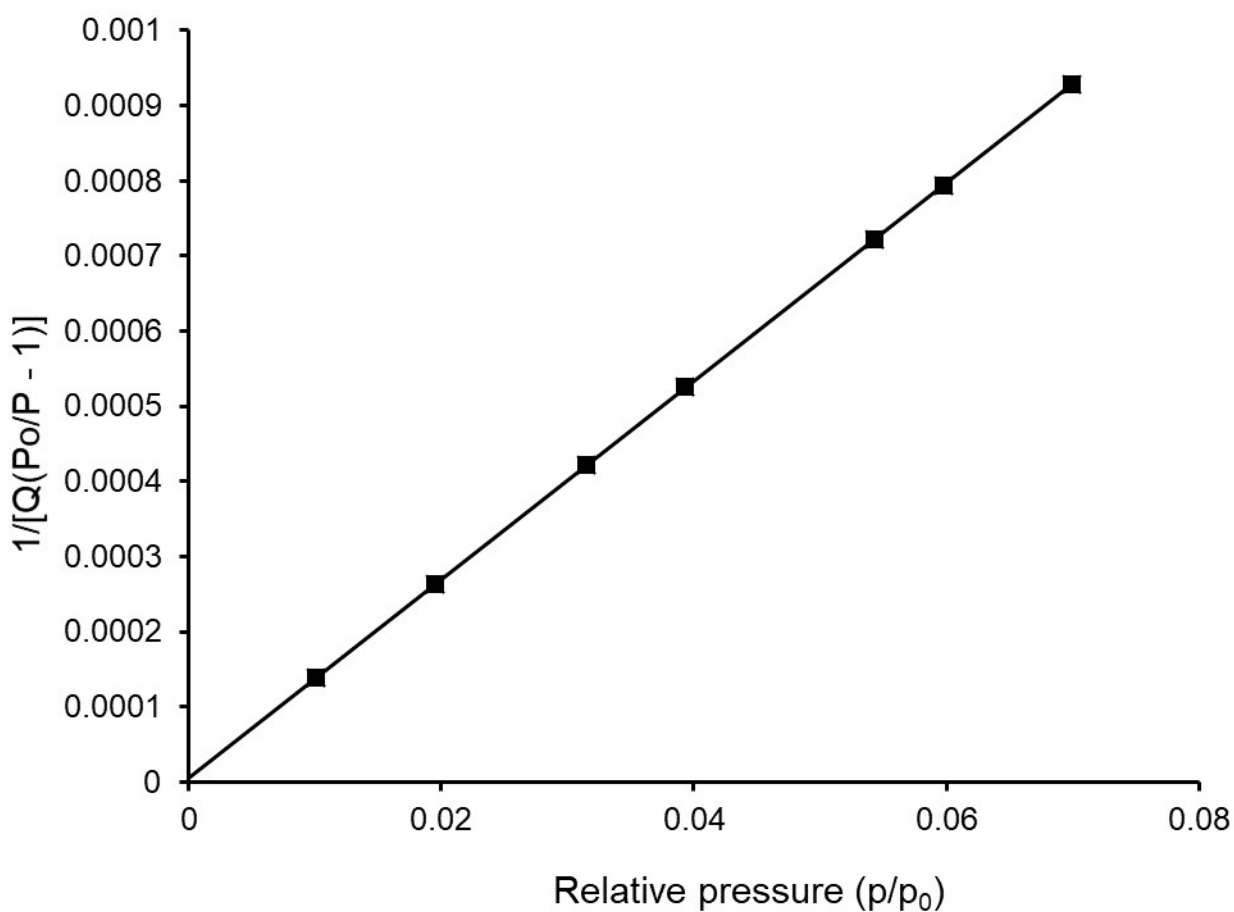
<sup>d</sup>School of Materials, University of Manchester, Oxford Road, Manchester M13 9PL, United  
Kingdom

<sup>e</sup>Electron Physical Sciences Imaging Centre, Diamond Light Source Ltd., Oxfordshire  
OX11 0DE, United Kingdom

<sup>f</sup>Department of Chemistry, University College London, 20 Gordon Street, London  
WC1H 0AJ, U.K., & Research Complex at Harwell, Rutherford Appleton Laboratory, Didcot  
OX11 0FA, U.K

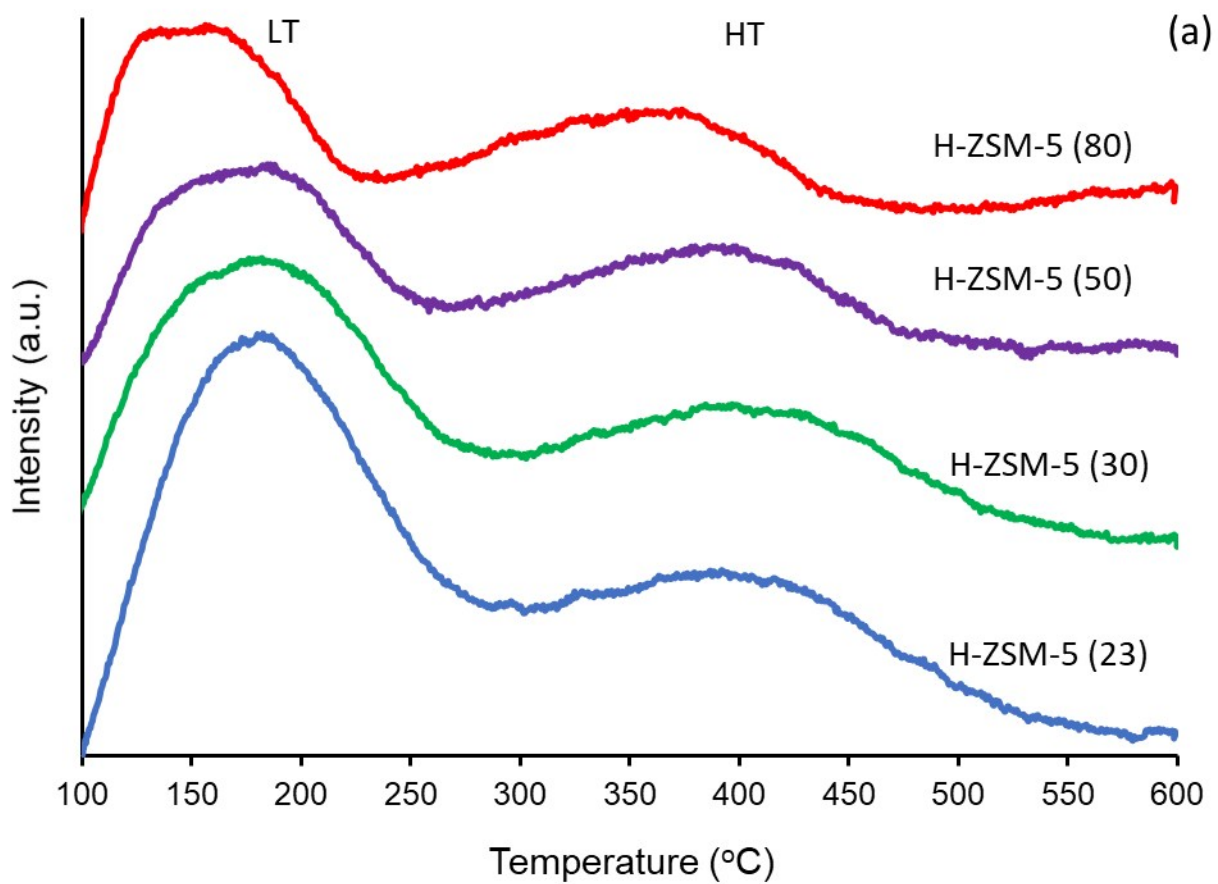
## ESI 1

The BET method is, in a strict sense, not applicable in the case of microporous adsorbents<sup>1,2</sup>. However, Rouquerol *et al.*<sup>3</sup> suggested a procedure to determine an appropriate  $p/p_0$  range for BET analysis of microporous materials. This procedure was utilized in this study to estimate the surface area of the ZSM-5 supports and the corresponding catalysts. Moreover, micropore volume and the concentration of Pd, Pt in the catalysts were analyzed using the t-plot and ICP-AES methods, respectively.



**Figure S1.** An example of the BET plot of the Pd,Pt,TiO<sub>2</sub>/H-ZSM-5 (80) catalyst utilizing only data in the low  $p/p_0$  region (less than 0.1). The y-intercept value here is 0.000006, which is positive and thus satisfies the most important requirement proposed by Rouquerol *et al.*

ESI 2 NH<sub>3</sub>-TPD



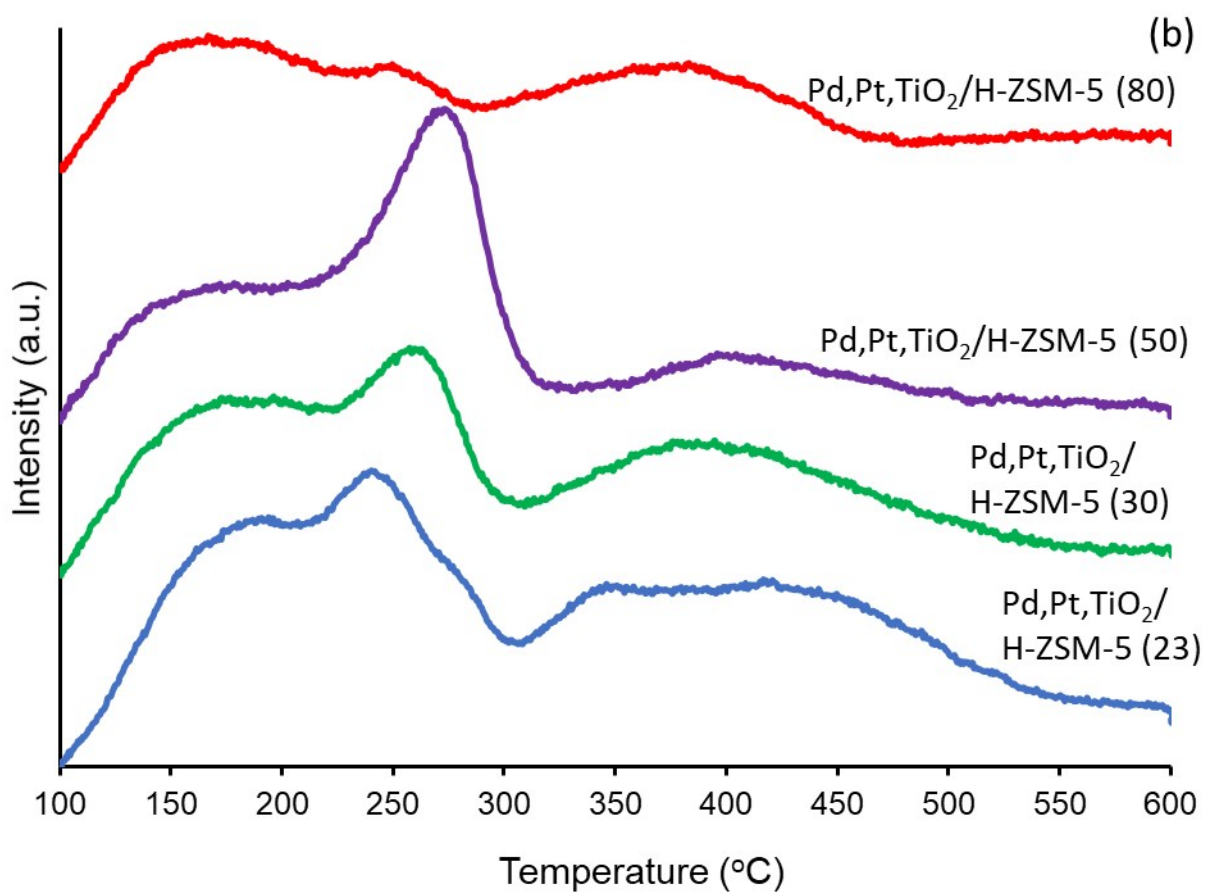


**Figure S2.** NH<sub>3</sub>-TPD profiles of (a) ZSM-5 supports and (b) the corresponding catalysts

### ESI 3

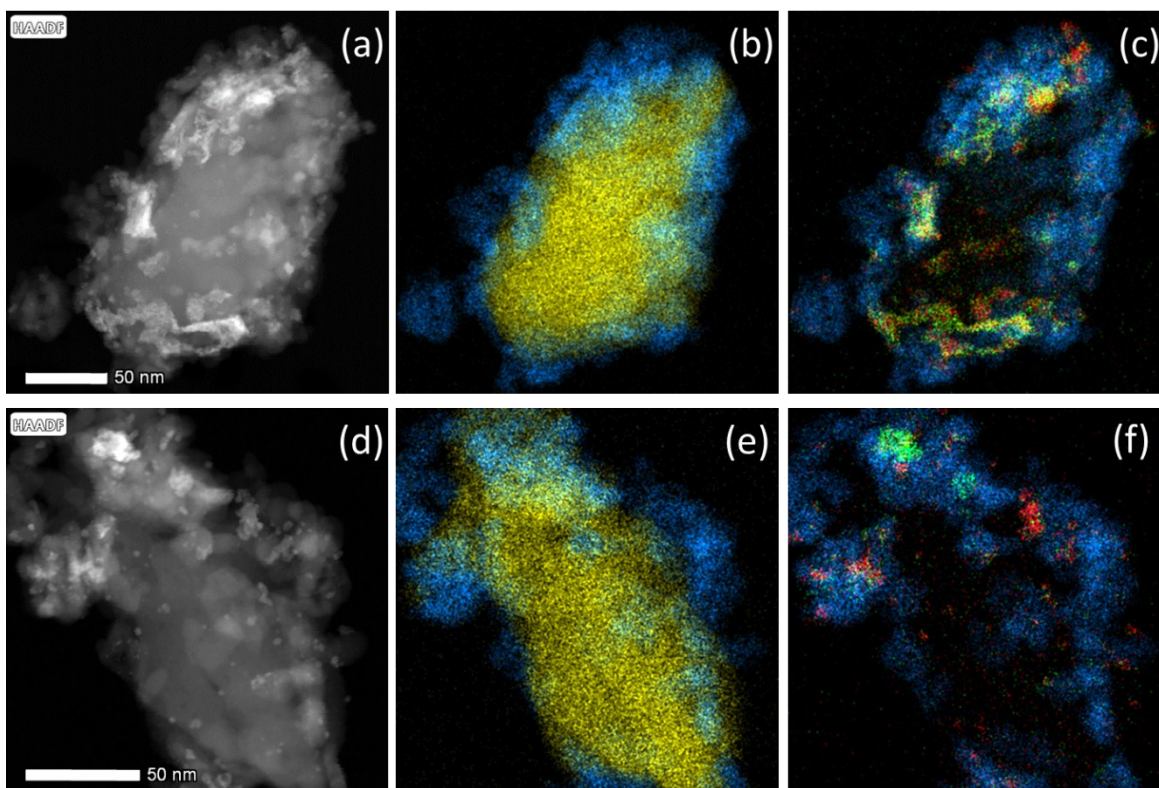


**Figure S3.** Scanning transmission electron microscope high angle annular dark field (STEM-HAADF) imaging (a and d). Energy dispersive X-ray spectroscopy (EDS) mapping elemental maps and overlays of Pd/Pt/TiO<sub>2</sub>/H-ZSM-5 (23) (b – c) and Pd/Pt/TiO<sub>2</sub>/H-ZSM-5 (80) (e – f). For Si (yellow) / Ti (blue) (b and e) and for Ti (blue) / Pd (red) / Pt (green) (c and f) with the yellow here indicating areas where the Pd and Pt are co-located.

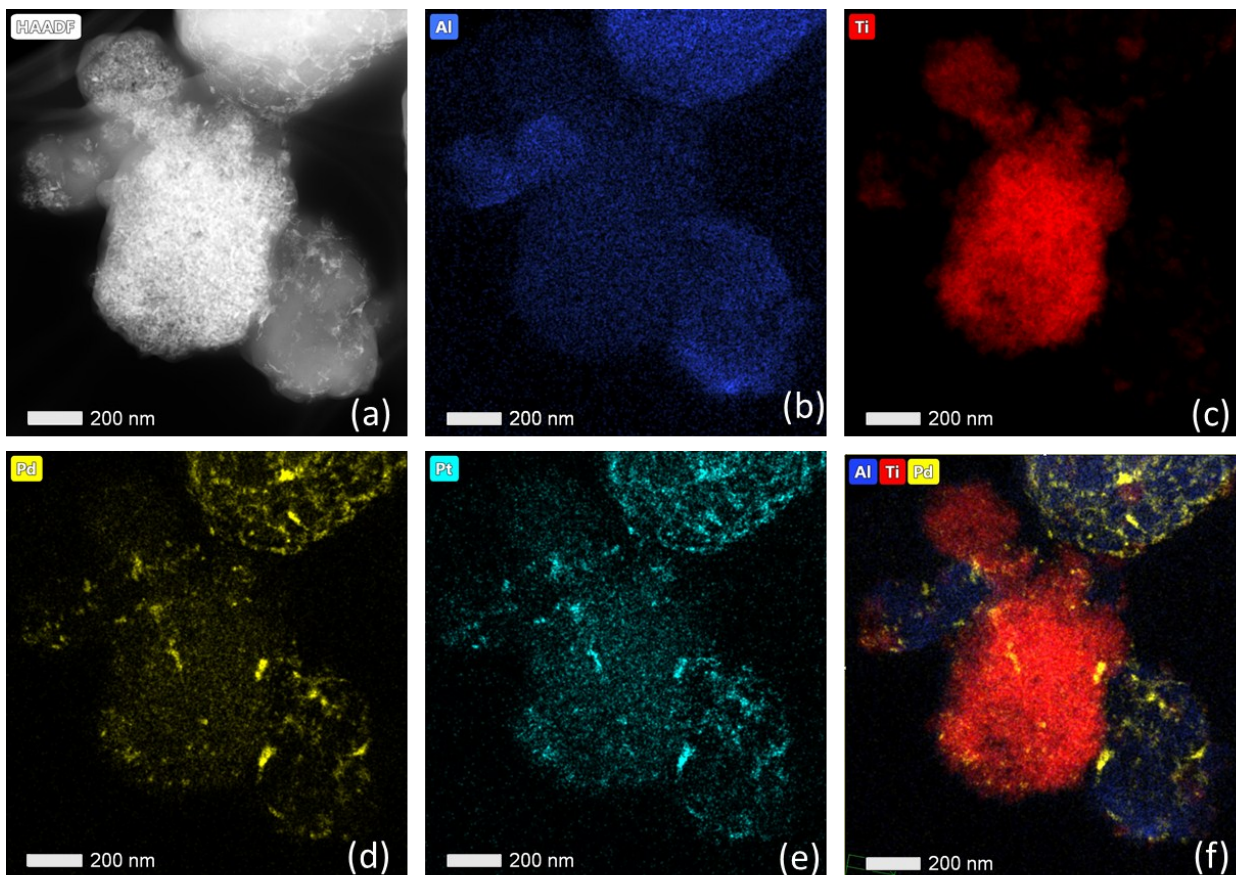


**Figure S4.** Scanning transmission electron microscope high angle annular dark field (STEM-HAADF) imaging (a) and energy dispersive X-ray spectroscopy (EDS) elemental maps of the Pd/Pt/TiO<sub>2</sub>/H-ZSM-5 (80) catalyst (b, c, d, e and f). The blue indicates Al, red Ti, yellow Pd and turquoise Pt.

## ESI 4

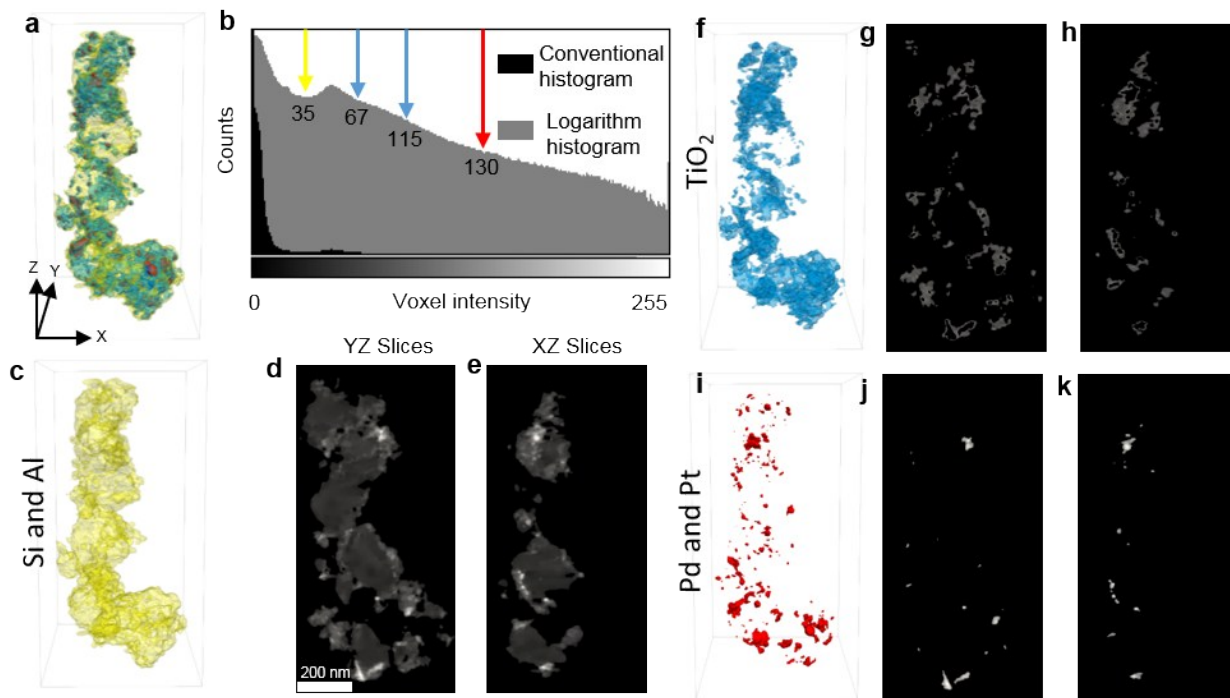


**Figure S5.** 3D visualisation and 2D orthoslices from a STEM-HAADF electron tomographic reconstruction of Pd/Pt/TiO<sub>2</sub>/H-ZSM-5 (23). a) 3D surface render of the reconstruction with colours to illustrate intensity differences, yellow, low HAADF intensity corresponding to Si and Al support, blue, intermediate intensity corresponding to TiO<sub>2</sub> particles, red, high intensity as Pd and Pt rich nanoparticles. b), histogram of the unprocessed reconstruction. Voxel intensities ranging from 35-255, 67-115 and 130-255 are represented as the yellow tomogram in c) the blue tomogram in f) and the red tomogram in i) respectively. d) and e), g) and h) and j) and k) are 2D slices extracted from c), f) and i), respectively.

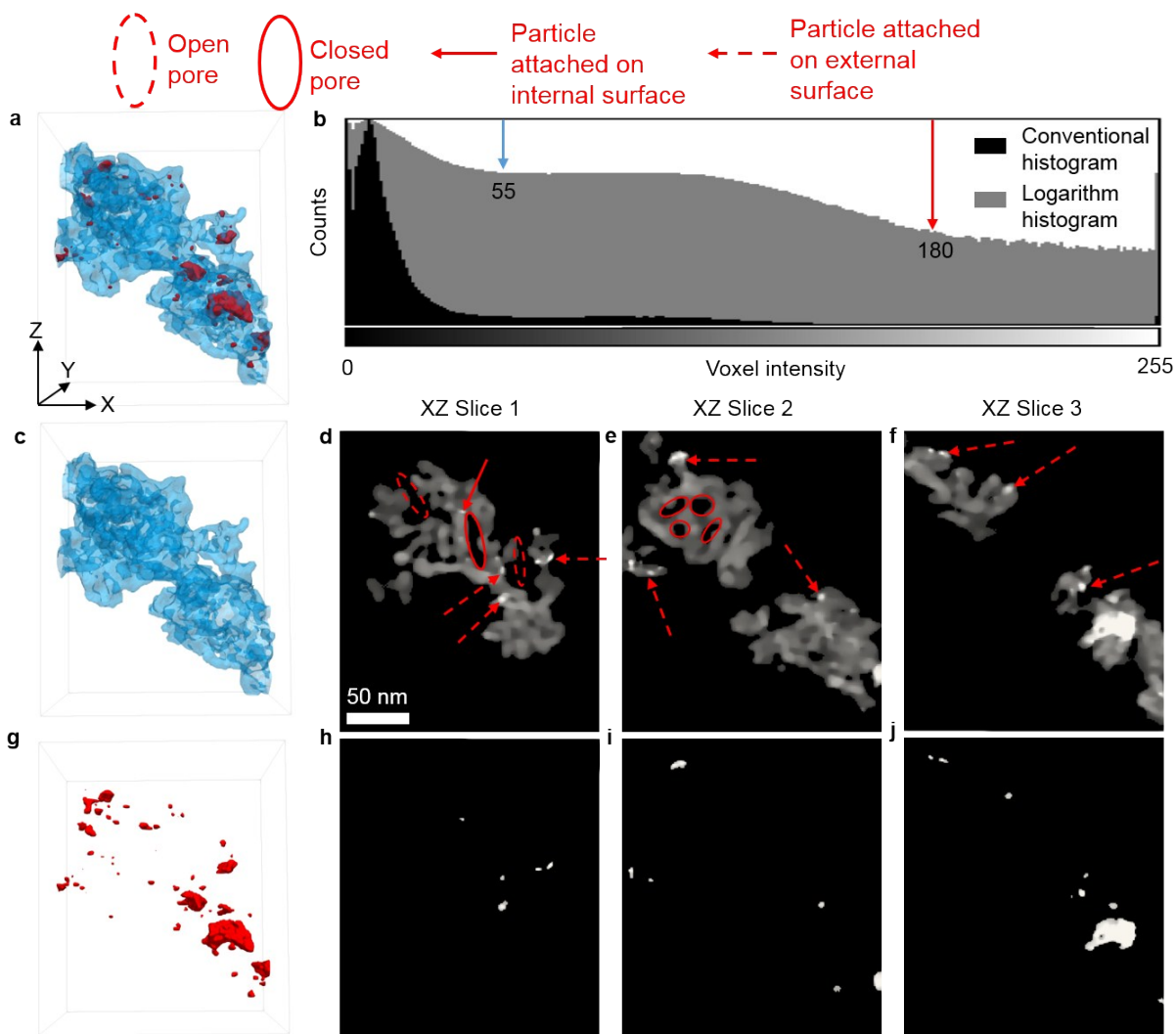


**Figure S6.** 3D visualisation and orthoslices from the STEM-HAADF electron tomographic reconstruction of Pd/Pt/TiO<sub>2</sub>/H-ZSM-5 (80). a) 3D surface render of the reconstruction with colours to illustrate intensity differences, blue, low HAADF STEM intensity corresponding to the TiO<sub>2</sub> support, red, high HAADF STEM intensity corresponding to the Pd and Pt rich nanoparticles. b) histogram of the unprocessed reconstruction. Voxel intensities ranging from 55-255 and 180-255 are represented as blue tomogram in c) and red tomogram in g) respectively. d-f) and h-j) are 2D slices extracted from c) and g) respectively. Legend at the top refers to the annotations on the 2D slices in d-f.

## ESI 5

### Fit at Pd K-edge

The co-ordination numbers (CNs) for the oxide reference were fixed as determined by its crystal structure. All other parameters, including the bond distances, and Debye–Waller factors were free to vary. Good fit was obtained for PdO, as suggested by the low R-factor. The refined bond lengths were consistent with PdO's crystal structure <sup>4</sup>, and all the other parameters were physically sensible. Thus, the same model was used to fit the three catalysts, which results in similarly good fits.

**Table S1.** Best-fit parameters obtained by fitting EXAFS data measured from PdO and the three catalysts at Pd K-edge

Sample	Shell	Co-ordination number	Bond length (Å)	Debye-Waller factor (Å <sup>2</sup> )	$\Delta E_0$ (eV)	R-factor
PdO	1 <sup>st</sup> (Pd-O)	4	2.02	0.0022	-0.9	0.009
	2 <sup>nd</sup> (Pd-Pd)	4	3.03	0.0043		
	3 <sup>rd</sup> (Pd-Pd)	8	3.42	0.0049		
Pd,Pt,TiO <sub>2</sub> /H-ZSM-5 (23)	1 <sup>st</sup> (Pd-O)	4.5	2.02	0.0024	-2.0	0.022
	2 <sup>nd</sup> (Pd-Pd)	5.0	3.06	0.0067		
	3 <sup>rd</sup> (Pd-Pd)	6.2	3.45	0.0063		
Pd,Pt,TiO <sub>2</sub> /H-ZSM-5 (50)	1 <sup>st</sup> (Pd-O)	4.5	2.02	0.0022	-2.0	0.020
	2 <sup>nd</sup> (Pd-Pd)	5.3	3.06	0.0066		
	3 <sup>rd</sup> (Pd-Pd)	6.5	3.45	0.0059		
Pd,Pt,TiO <sub>2</sub> /H-ZSM-5 (80)	1 <sup>st</sup> (Pd-O)	4.4	2.02	0.0022	-1.7	0.020
	2 <sup>nd</sup> (Pd-Pd)	5.4	3.06	0.0065		
	3 <sup>rd</sup> (Pd-Pd)	6.3	3.45	0.0059		

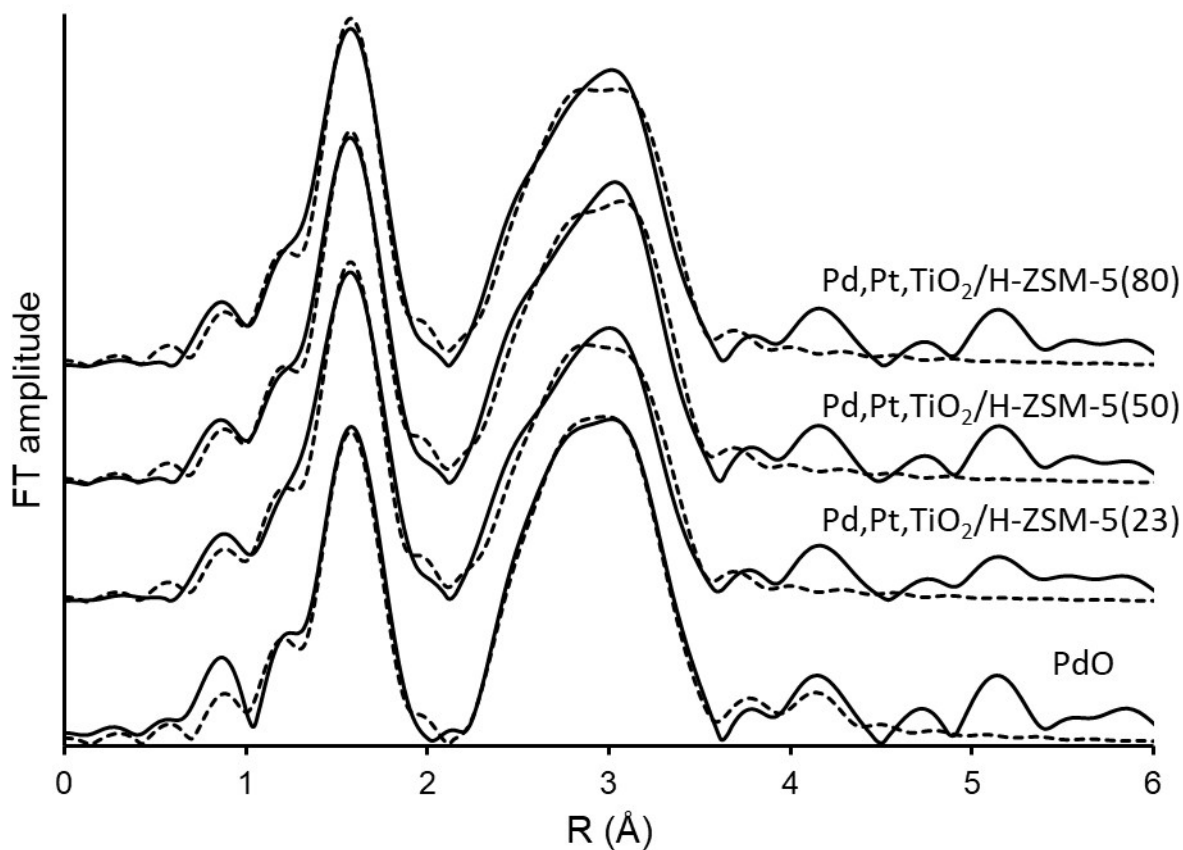


**Figure S7.** Experimental EXAFS data (solid line) obtained with PdO reference and the three catalysts and the corresponding fitted model from FEFF (dashed line). Data obtained at the Pd K-edge.

#### Fit at Pt L<sub>III</sub>-edge

In this fit, it was necessary to fix the Debye–Waller factor in the 3<sup>rd</sup> and 4<sup>th</sup> shells to 0.003 and 0.006, respectively, as physically meaningful values could not be obtained when this parameter was free to vary. This results in a good fit with a R-factor of 0.01.

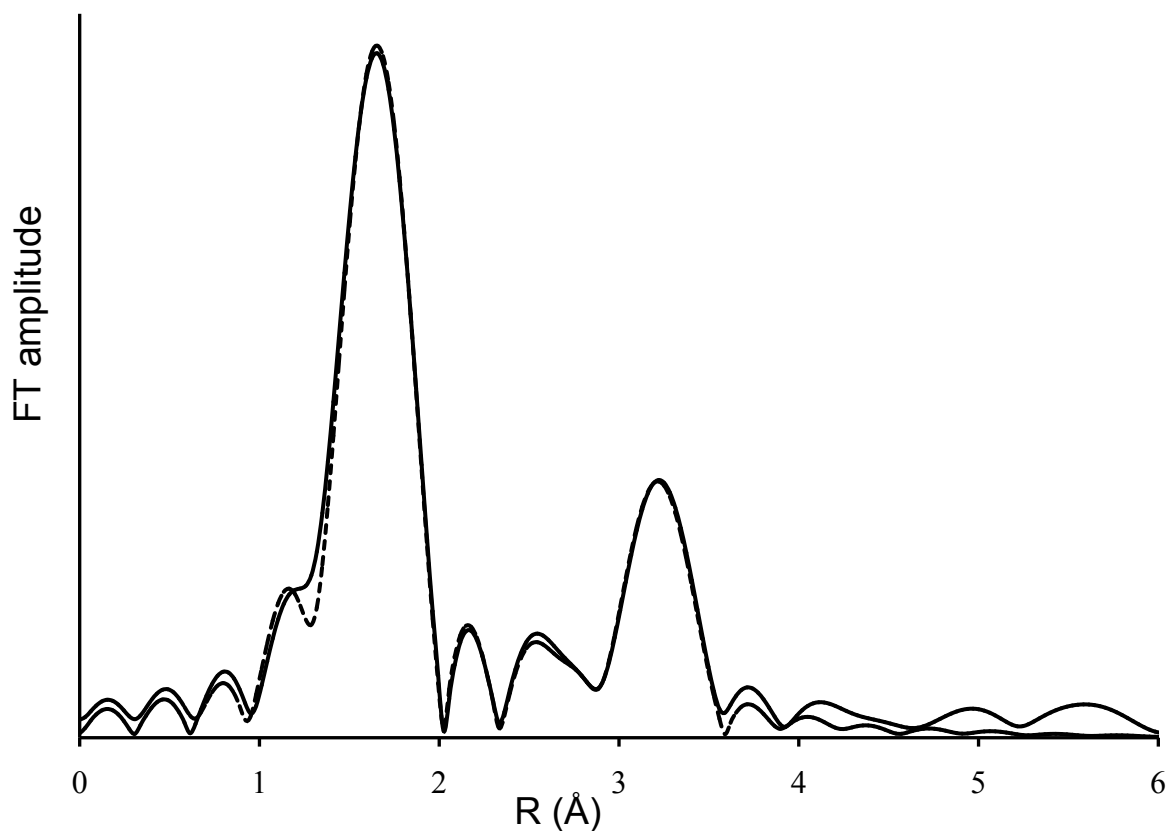


**Figure S8.** Experimental EXAFS data (solid line) and fitted model (dash line) for Pd,Pt,TiO<sub>2</sub>/HZSM-5 (23). Data obtained at the Pt L<sub>III</sub>-edge.

**Table S2.** Best-fit parameters obtained by fitting EXAFS data measured from Pd,Pt,TiO<sub>2</sub>/H-ZSM-5 (23) at the Pt L<sub>III</sub>-edge.

Sample	Shell	Co-ordination number	Bond length (Å)	Debye-Waller factor (Å <sup>2</sup> )	$\Delta E_0$ (eV)	R-factor
PtO <sup>a</sup>	1 <sup>st</sup> (Pt-O)	4	2.02			
	2 <sup>nd</sup> (Pt-Pt)	4	3.04			
	3 <sup>rd</sup> (Pt-Pt)	8	3.43			
	4 <sup>th</sup> (Pt-O)	8	3.65			
Pd,PtTiO <sub>2</sub> /H-ZSM-5 (23)	1 <sup>st</sup> (Pt-O)	3.5	2.02	0.0018	12.8	0.01
	2 <sup>nd</sup> (Pt-Pt)	1.2	3.00	0.0063		
	3 <sup>rd</sup> (Pt-Pt)	1.0	3.47	0.006 <sup>b</sup>		
	4 <sup>th</sup> (Pt-O)	5.4	3.63	0.003 <sup>b</sup>		

<sup>a</sup>Data from crystallography. <sup>b</sup>fixed

## ESI 6

**Table S3.** Position of the Pd and Pt peaks in eV in XPS analysis

Sample	Pd 3d <sub>5/2</sub>	Pd3d <sub>3/2</sub>	Pt 4f <sub>5/2</sub>	Pt 4f <sub>7/2</sub>
Pd,Pt,TiO <sub>2</sub> /H-ZSM-5 (23)	337.18	342.58	75.58	72.18
Pd,Pt,TiO <sub>2</sub> /H-ZSM-5 (50)	337.08	342.28	75.48	72.08
Pd,Pt,TiO <sub>2</sub> /H-ZSM-5 (80)	336.68	342.18	75.18	71.88

ESI 7

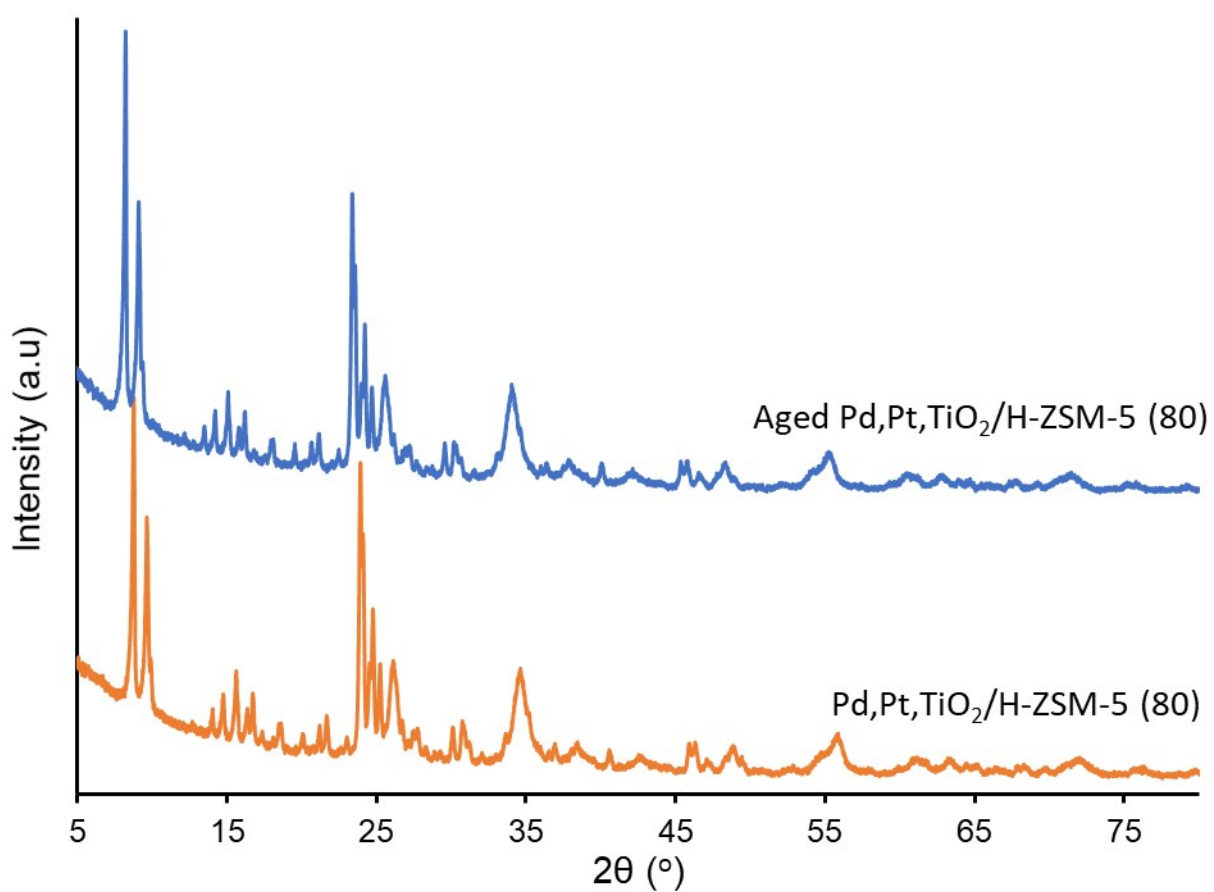


**Figure S9.** XRD diffractogram of Pd,Pt,TiO<sub>2</sub>/H-ZSM-5 (80) and the same material after 50 h time on stream.

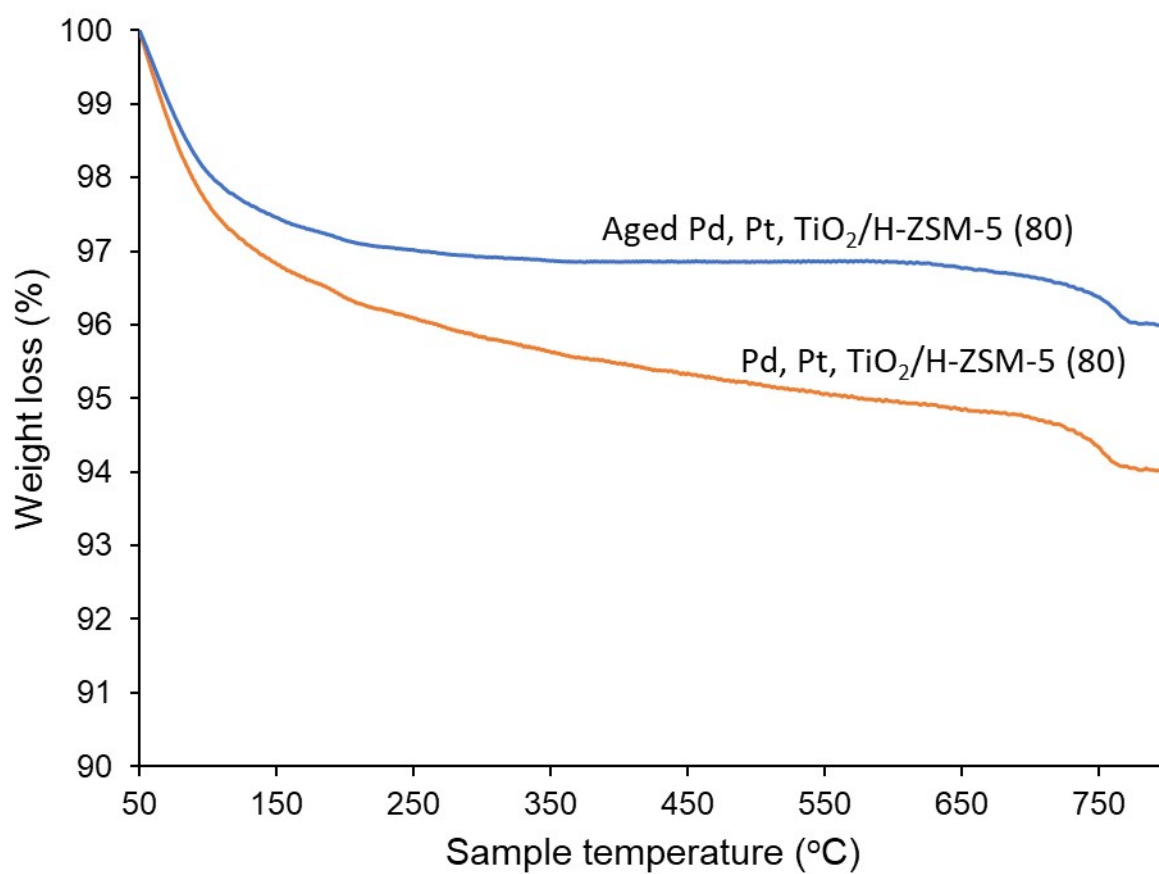


**Figure S10.** TGA analyses in O<sub>2</sub>

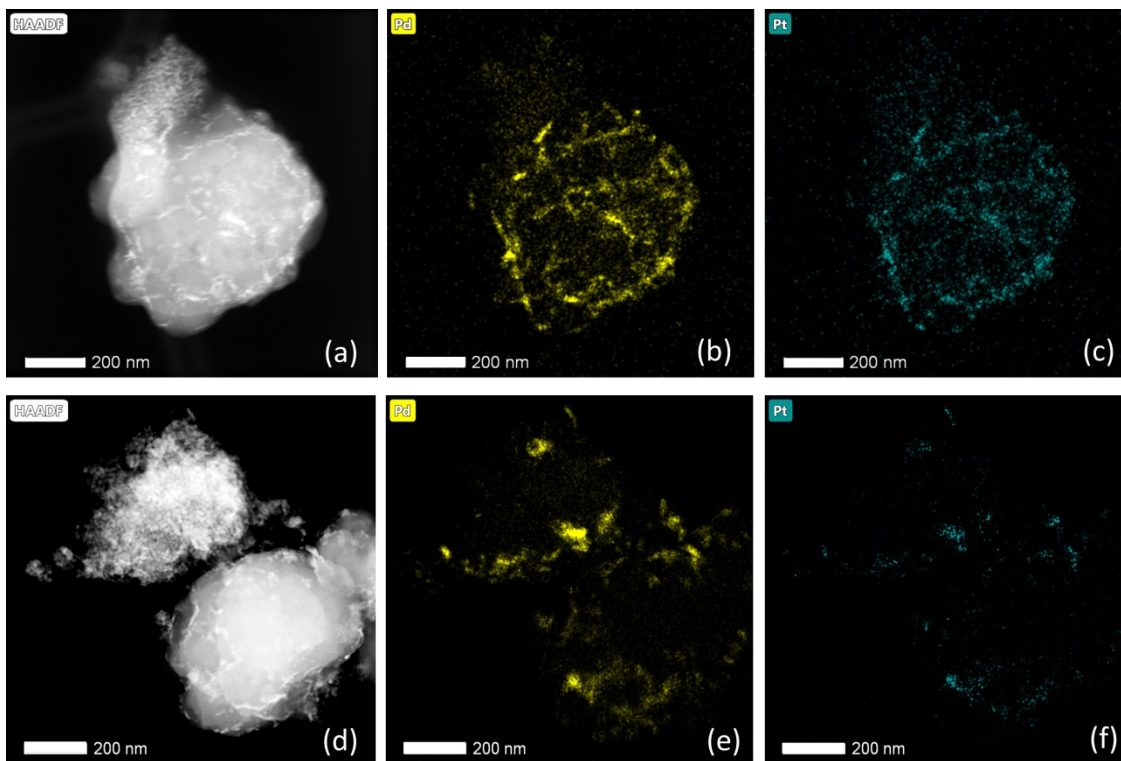


**Figure S11.** STEM-HAADF images and EDS Pd (yellow), Pt (turquoise) element mapping of (a-c) the original and (d-f) the aged Pd,Pt,TiO<sub>2</sub>/H-ZSM-5 (80).

ESI 8

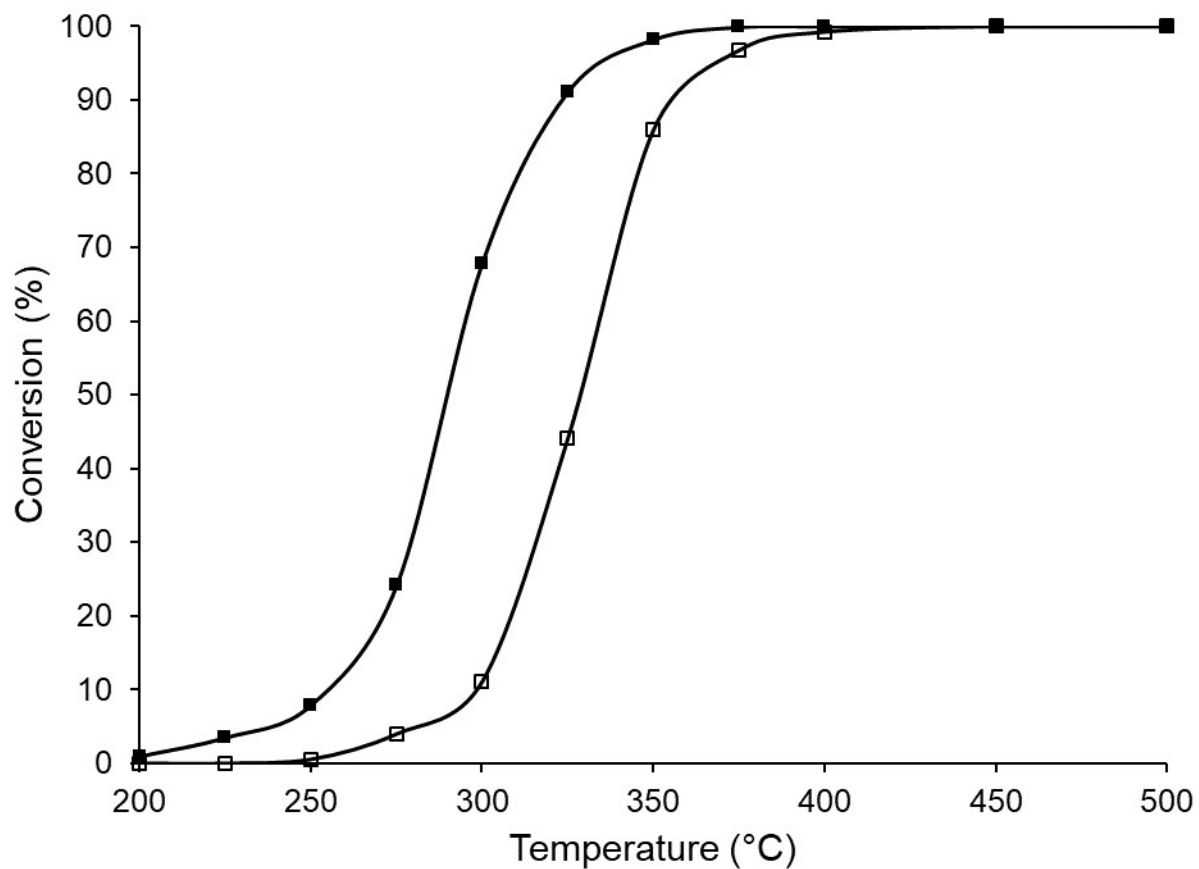


**Figure S12.** Catalytic activity profiles for methane oxidation under dry conditions (closed symbols) and in the presence of 9 mL min<sup>-1</sup> water (open symbols) for Pd,Pt,TiO<sub>2</sub>/H-ZSM-5 (80). Nominal composition: 5 wt.% Pd, 2 wt.% Pt, 17.5 wt.% TiO<sub>2</sub> on 75.5 wt.% zeolite.

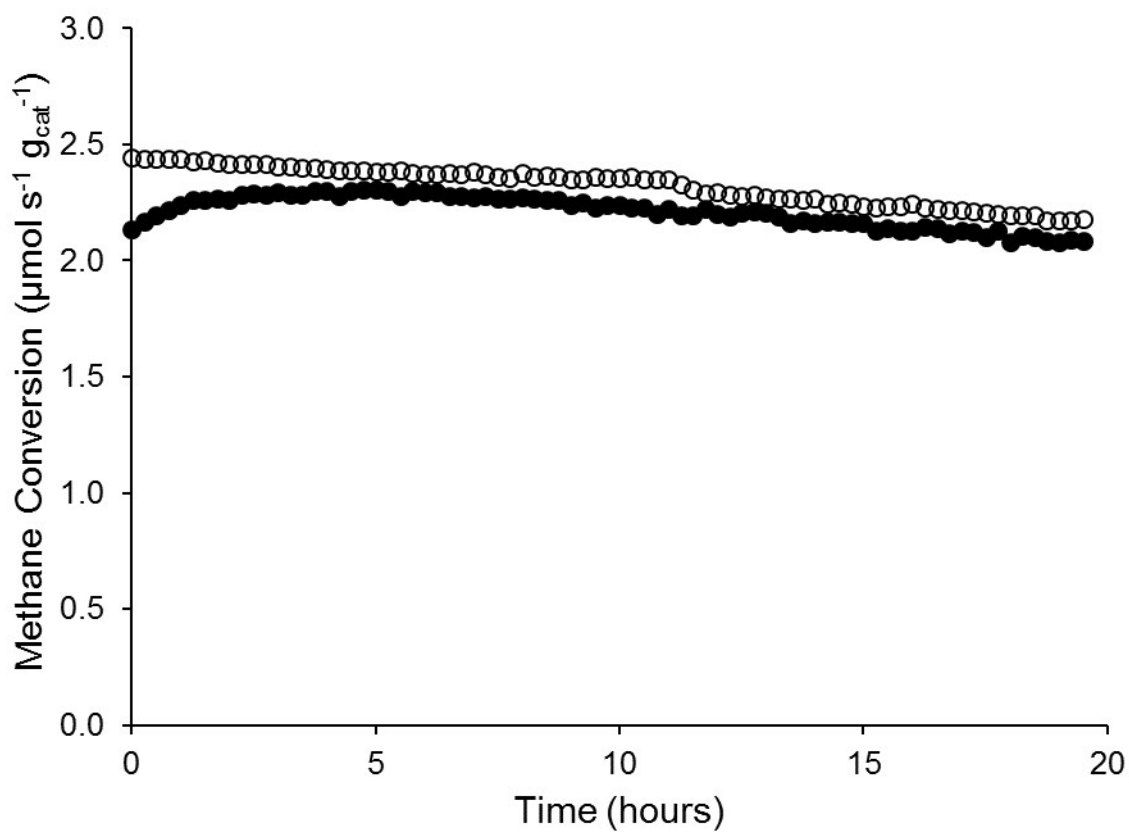


**Figure S13.** Comparison of the stability of Pd,Pt,TiO<sub>2</sub>/ZSM-5 (80) under dry conditions at 300 °C (closed symbols) and in the presence of 9 mL min<sup>-1</sup> water at 350 °C (open symbols).

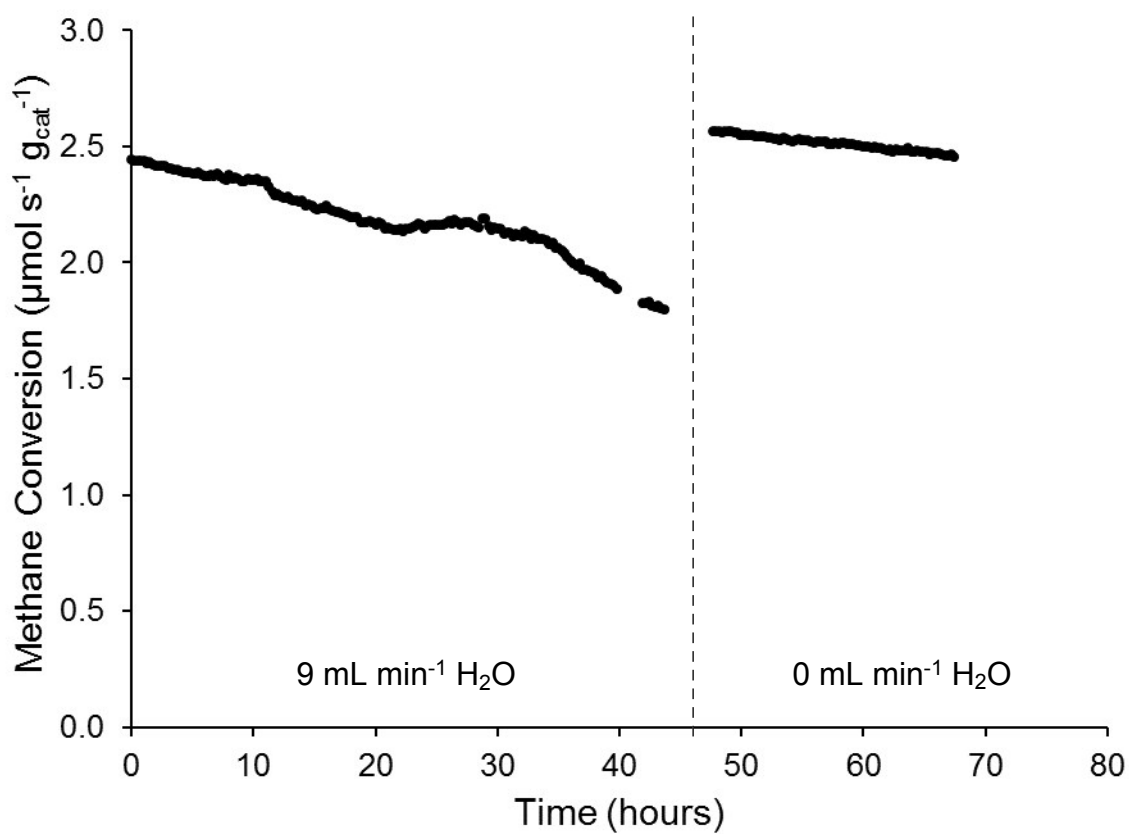


**Figure S14.** Stability of catalyst Pd,Pt,TiO<sub>2</sub>/H-ZSM-5 (80) with 9 mL min<sup>-1</sup> water in the feed and when water is removed at 350 °C. Feed composition: 0.9 mL min<sup>-1</sup> CH<sub>4</sub>, 18 mL min<sup>-1</sup> O<sub>2</sub>, 9 mL min<sup>-1</sup> Ne and either 9 or 0 mL min<sup>-1</sup> H<sub>2</sub>O with 152.1 mL min<sup>-1</sup> Ar.

## References

- [1] J.S. S. Lowell, M. A. Thomas, and M. Thommes, *Characterization of Porous Solids and Powders: Surface Area, Porosity, and Density*, Springer 2004.
- [2] R. Haul, S. J. Gregg, K. S. W. Sing: *Adsorption, Surface Area and Porosity*. 2. Auflage, Academic Press, London 1982. 303 Seiten, Preis: \$ 49.50, *Berichte der Bunsengesellschaft für physikalische Chemie*, 86 (1982) 957-957.
- [3] J. Rouquerol, P. Llewellyn, F. Rouquerol, Is the BET equation applicable to microporous adsorbents?, in: P.L. Llewellyn, F. Rodriguez-Reinoso, J. Rouquerol, N. Seaton (Eds.) *Studies in Surface Science and Catalysis*, Elsevier 2007, 49-56.
- [4] A. Ali, W. Alvarez, C.J. Loughran, D.E. Resasco, State of Pd on H-ZSM-5 and other acidic supports during the selective reduction of NO by CH<sub>4</sub> studied by EXAFS/XANES, *Applied Catalysis B: Environmental*, 14 (1997) 13-22.